

**Relation between  $^{207}\text{Pb}$  NMR chemical shift and the morphology and crystal structure for the apatites  $\text{Pb}_5(\text{AO}_4)_3\text{Cl}$ , vanadinite ( $\text{A} = \text{V}$ ), pyromorphite ( $\text{A} = \text{P}$ ), and mimetite ( $\text{A} = \text{As}$ )**

Otto E. O. Zeman<sup>a</sup>, Rupert Hochleitner<sup>b</sup>, Wolfgang W. Schmahl<sup>b,c</sup>, Konstantin Karaghiosoff<sup>a</sup>,

Thomas Bräuniger<sup>a,\*</sup>

July 21, 2020

**Revision #1**

<sup>a</sup> Department of Chemistry, University of Munich (LMU), Butenandtstr. 5-13, 81377 Munich, Germany

<sup>b</sup> Mineralogical State Collection Munich (SNSB), Theresienstr. 41, 80333 Munich, Germany

<sup>c</sup> Department of Earth and Environmental Sciences, Section Crystallography, University of Munich (LMU), Theresienstr. 41, 80333 Munich, Germany

**Corresponding Author**

\* Tel. +49-89-2180-77433. E-mail: [thomas.braeuniger@cup.lmu.de](mailto:thomas.braeuniger@cup.lmu.de)

## Abstract

In this paper, we discuss information on crystal structure and morphology available from Nuclear Magnetic Resonance (NMR) spectroscopy of  $^{207}\text{Pb}$  for the mineral family  $[\text{Pb}(4f)]_2[\text{Pb}(6h)]_3(\text{AO}_4)_3\text{Cl}$  with  $A = \text{V}$  (vanadinite),  $\text{P}$  (pyromorphite), and  $\text{As}$  (mimetite). The isotropic chemical shift of the  $^{207}\text{Pb}$  atoms at Wyckoff positions  $4f$  and  $6h$  was (re-)determined from either static single-crystal or magic-angle spinning NMR experiments. This isotropic shift can be linearly correlated to the unit cell volume within the mineral family, and in the wider context of lead-bearing minerals, to the shortest  $\text{Pb—O}$  distance for position  $4f$ , in which  $^{207}\text{Pb}$  is solely coordinated by oxygen. By evaluating the number of resonances and their respective line widths in the  $^{207}\text{Pb}$ -NMR spectra of these three naturally grown minerals, it could be established that vanadinite forms single-domain macroscopic crystals with very small mosaicity, whereas pyromorphite crystals show NMR characteristics which can be interpreted as being caused by significant mosaicity. In some instances, this mosaic spread could be quantitatively approximated by a Gaussian distribution with a standard deviation angle of  $\sigma = 5^\circ$ . In contrast, our mimetite specimen were composed of multiple sub-crystals with a very a high variability of orientations, going beyond mere mosaicity effects. By extending  $\square$  the NMR methodology presented here to other minerals, it may be possible to gain new insights about structure-property relationships and the morphology of natural grown minerals.

## Introduction

Nuclear magnetic resonance has proven itself as a powerful tool to obtain reliable structural information on a local (atomic) length scale, notably where structural disorder or amorphous structural states make the application of X-ray diffraction very difficult (Laws et al. 2002, MacKenzie and Smith 2002). Beyond the atomic scale structure, which is largely determined by P-T-conditions and the time-traverse through P-T-space, parameters such as supersaturation, stresses, defect accumulation or ion transport during crystal growth and crystal deformation also print their stamp on crystal morphology (Chopard et al. 1991, Penn and Banfield 1999), size (Galwey and Jones 1963, Otolara and Garcia-Ruiz 2014), mosaicity and microstructure (Vinet et al. 2011). While the latter structural aspects are rarely addressed by NMR techniques, some information on these aspects may be available also *via* solid-state NMR, as will be shown in the current work.

Generally, NMR spectroscopy probes the response of nuclear spins in an external magnetic field, with the response being modified by the electronic surroundings (the so-called chemical shift and, for spin  $I > \frac{1}{2}$ , quadrupolar coupling). NMR is therefore capable of delivering information about the distribution of electrons and nuclei in the crystal structure, and in some cases, even distance information by evaluating interaction between neighboring spins, the so-called direct and/or indirect coupling. The main aim of “NMR Crystallography” is to establish correlations between NMR parameters and structural features, such as bond lengths or bond angles. One such parameter is the isotropic chemical shift  $\delta_{iso}$  of the NMR resonance, which however is defined as the weighted sum of three components (the diagonal elements of the second-rank tensor  $\delta$ , as discussed in detail below):

$$\delta_{iso} = \frac{1}{3} \sum_i \delta_{ii} \quad (1)$$

It is comparatively easy to determine the isotropic chemical shift for nuclei with spin  $I = \frac{1}{2}$ , by acquiring magic-angle spinning (MAS) spectra of a powdered sample, and identifying the isotropic peak (Andrew 1981). The value of  $\delta_{iso}$  can then be utilized to derive important structural information such as number and type of atoms coordinating the observed nuclide (Harris 2004). The structural environment has a particularly strong effect on  $\delta_{iso}$  for heavy nuclides (such as  $^{119}\text{Sn}$ ,  $^{199}\text{Hg}$  or  $^{207}\text{Pb}$ ), due to their high number of electrons (Harris and Sebal 1987). We have recently conducted NMR studies of  $^{207}\text{Pb}$  ( $I = \frac{1}{2}$ ) on naturally grown single crystals of pyromorphite (Zeman et al. 2017), and vanadinite (Zeman et al. 2018), determining both the full chemical shift tensor and the isotropic shift. In the current work, we also include NMR results of mimetite. All three compounds are secondary minerals, occurring in the oxidized zones of lead deposits, and have recently attracted attention for their ability to immobilize heavy metal ions (see for example, Epp et al. 2019, and references therein). The general formula of the minerals, all of which belong to the apatite supergroup and crystallize in space group  $P6_3/m$  (Okudera 2013), may be written as  $[\text{Pb}(4f)]_2[\text{Pb}(6h)]_3(\text{AO}_4)_3\text{Cl}$ , with  $Z = 2$ , and  $A = \text{V}$  (vanadinite),  $\text{P}$  (pyromorphite), and  $\text{As}$  (mimetite). In all crystal structures, the lead atom at Wyckoff position  $4f$  is located on a  $6_3$  screw axis with two pairs of magnetically inequivalent  $^{207}\text{Pb}$  sites, whereas lead at position  $6h$  is located on a mirror plane, giving three pairs of magnetically inequivalent  $^{207}\text{Pb}$  sites per unit cell.

When comparing our NMR results for these three isostructural minerals, we found an expected relation of the isotropic shift  $\delta_{iso}$  to the unit cell volume within this mineral family. Also, in the wider context of lead-bearing minerals, the  $\delta_{iso}$  values agree well with a previously suggested relation (Zeman et al. 2019) to the shortest Pb-O distance, for  $\text{Pb}^{2+}$  ions which are coordinated solely by oxygen. In contrast to pyromorphite and vanadinite, we did however not succeed in determining the full chemical shift tensor for mimetite using the established methodology of

single-crystal NMR spectroscopy. This was due to the morphology of the available minerals: even very tiny specimen, which under the microscope appeared to be single crystals, were actually composed of multiple crystals, with their relative orientations showing a variation much greater than those expected from mosaicity effects. This prompted us to re-examine our data on vanadinite and pyromorphite, and in particular an orientation-dependent line broadening we had observed in the NMR spectra of the latter. As described in the second part of the paper, a clear trend in crystal morphology of the three isostructural minerals may be discerned, and partly even quantitatively estimated, from single-crystal NMR experiments: Whereas our vanadinite specimens show a high degree of crystallinity, pronounced mosaicity effects are present in pyromorphite, while the high variability of domain orientations goes beyond mere mosaicity in mimetite. To some extent, these findings are mirrored in the appearance of the minerals. While crystals of vanadinite mostly occur with well-defined hexagonal crystal faces and in uniform red color (see Fig. 1a), pyromorphite (Fig. 1b), and mimetite (Fig. 1c) can be found in crystals with widely varying morphology and color. Thus, in this work, we aim to show that the benefits of single-crystal NMR may extend beyond the mere determination of NMR interaction parameters, but in certain cases also supply information about internal structure and morphology of the studied crystals.

## Results and Discussion

### Determination of the $^{207}\text{Pb}$ chemical shift from single crystalline or polycrystalline material

To describe the NMR response of a nuclide with spin  $I = \frac{1}{2}$ , such as  $^{207}\text{Pb}$ , one considers the general Hamiltonian  $\hat{H}_{\text{NMR}}$  (see, for example, Laws et al. 2002), which determines the spin energy levels in an external magnetic field  $\vec{B}_0$ :

□

□

$$\hat{H}_{NMR} = -\gamma_n \hat{B}_0 \hat{I}_z - \gamma_n \hat{B}_0 \delta \hat{I} + \sum_i \hat{I}_i \cdot D \cdot \hat{I}_i \quad (2)$$

Here, the first term is the nuclear Zeeman interaction, which for a nuclide with gyromagnetic ratio  $\gamma_n$  provides the resonance (Larmor) frequency  $\nu_0$ , and scales with the strength of the external field  $\hat{B}_0$ . The third term describes the interactions between the nuclear magnetic moments in the crystal structure. For the compounds discussed here, these spin couplings result only in a general broadening of the resonance lines, which will be discussed in more detail below, in the context of crystal mosaicity.

The second term in Eq. (2) describes the modification of this interaction by the diamagnetic electron cloud surrounding the nucleus, the so-called chemical shift. In solids, the chemical shift is orientation dependent, and therefore described by a second-rank tensor  $\delta$ , of which only the symmetric part is considered, because the anti-symmetric part is practically unobservable (Anet and O'Leary 1991). The relation between electron distribution and crystal structure is most evident when expressing the chemical shift (CS) tensor  $\delta$  in the frame of the crystal lattice (*CRY*), which here we choose to be the *a\*bc* system of the hexagonal unit cell. In this frame, the CS tensor takes the form:

$$\delta^{CRY} = \begin{pmatrix} \delta_{a^*a^*} & \delta_{a^*b} & \delta_{a^*c} \\ \delta_{a^*b} & \delta_{bb} & \delta_{bc} \\ \delta_{a^*c} & \delta_{bc} & \delta_{cc} \end{pmatrix} \quad (3)$$

The actual position of the resonance line now depends on the orientation of the magnetic field vector  $\hat{B}_0$  in the *CRY* frame, or in an alternative view, the orientation of the single crystal in the magnetic field, as described by the second term in Eq. (2). Due to the high number of electrons in heavy nuclides, such as lead, their NMR chemical shift is very sensitive to the structural environment, and the inherent orientation dependency is comparatively strong (Harris and Sebold 1987).

Most NMR measurements are performed on polycrystalline (“powder”) samples. Partly, this is due to the lack of sufficiently large single crystals, partly this may be traced to methodological aspects of single-crystal NMR, some of which are discussed in detail in (Zeman et al. 2019). If the number of crystallites in such a powder sample is large, all orientations of the CS tensor will be present simultaneously, resulting in a broad powder line shape, such as those displayed in Fig. 2. The static powder spectrum for  $^{207}\text{Pb}$  of pyromorphite shows a complex powder line shape (see Fig. 2a), resulting from the respective contributions of the lead atoms at the two Wyckoff positions  $6h$  and  $4f$ , as shown in Fig. 2b. To remove the broadening and regain resolution, the magic angle spinning (MAS) technique may be employed (Andrew 1981). In the limit of fast spinning, only one resonance line at position  $\delta_{iso}$  will remain for each crystallographic non-equivalent nuclide  $k$ . The highest spinning speed currently commercially available is about 110 kHz, and would be in principle sufficient to reduce the MAS spectra of pyromorphite to only the two isotropic bands with a relative intensity of 3:2 for position  $6h$  and  $4f$ , as may be seen from Fig. 2c. In the more common case of incomplete averaging, a spinning side band (SSB) manifold remains which for low spinning rates traces out the shape of the powder pattern, see Fig. 2d. By acquiring and analyzing MAS spectra at various spinning rates, a good estimate of the CS tensor  $\delta$  may be obtained (Herzfeld and Berger 1980). However, the most precise way to determine the tensor  $\delta$  is to perform NMR experiments on single crystals, which also supply  $\delta_{iso}$  via Eq. (1).

For both pyromorphite and vanadinite, we have determined the isotropic shifts of  $^{207}\text{Pb}$  by such single-crystal experiments, and used the values from MAS spectra only for verification (Zeman et al. 2017, Zeman et al. 2018). Because of the multi-domain structure of its crystals, single-crystal NMR is not feasible for mimetite,  $\text{Pb}_5(\text{AsO}_4)_3\text{Cl}$ , as will be discussed in more detail below. The hitherto unknown  $^{207}\text{Pb}$  isotropic shifts of mimetite were therefore derived from MAS spectra

only, such as the one displayed in Fig. 3. (Note that the severe overlap of the  $6h$  and  $4f$  signals in SSB manifold prevented us from estimating the full tensor by Herzfeld-Berger analysis.)

## Relation of the $^{207}\text{Pb}$ isotropic chemical shift to parameters of the crystal structure

The  $^{207}\text{Pb}$  isotropic chemical shifts of the three isostructural minerals  $[\text{Pb}(4f)]_2[\text{Pb}(6h)]_3(\text{AO}_4)_3\text{Cl}$  with  $A = \text{V}, \text{P}, \text{and As}$ , determined from either single-crystal or MAS NMR experiments, are listed in Table 1.

$\delta_{iso}$	Vanadinite	Pyromorphite	Mimetite
$6h$	$(-1729 \pm 9) \text{ ppm}$	$(-2170 \pm 8) \text{ ppm}$	$(-2074 \pm 3) \text{ ppm}$
$4f$	$(-1619 \pm 2) \text{ ppm}$	$(-2813 \pm 11) \text{ ppm}$	$(-2124 \pm 3) \text{ ppm}$

**Table 1.** Isotropic chemical shift of  $^{207}\text{Pb}$  at the position  $6h$  and  $4f$  in the apatite structure of vanadinite (from single-crystal NMR, Zeman et al. 2018), pyromorphite (from single-crystal NMR, this work) and mimetite (from MAS spectra, this work).

We can now proceed to test whether  $\delta_{iso}$  can be correlated to structural parameters within this mineral family. Such correlations have previously shown to be useful for deducing coordination numbers from chemical shift values. Usually, the chemical shift decreases with higher coordination, i.e. higher electron density, which translates into higher shielding values (MacKenzie and Smith 2002). Indeed we find a similar trend for our apatite minerals when plotting the chemical shift versus the ratio of the unique  $c$ -axis to the  $a$ -axis. As may be seen from Fig. 4, the chemical shift decreases when reducing the  $c/a$  ratio, which is equivalent to shrinking the unit cell volume and hence increasing the electron density.<sup>2</sup>



<sup>2</sup> In this argument, we do not take into account the different electron contributions of the central atom (V, P, or As) of the  $\text{AO}_4$  anion, since this atom is effectively screened by the surrounding oxygen atoms.

Furthermore, for  $\text{Pb}^{2+}$  ions solely coordinated by oxygen, it has recently been shown that the isotropic chemical shift correlates well with the shortest Pb—O distance within the coordination sphere (Zeman et al. 2019). The newly determined value of  $\delta_{iso}$  for the 4f lead atoms in the mimetite structure (which are only coordinated by oxygen) fits reasonably well into this correlation, without altering slope or intercept of the previously published linear fit (see Fig. S1 in the Supplementary Information).

#### **Determination of the full $^{207}\text{Pb}$ chemical shift tensor from single crystal experiments**

As already stated above, the most precise way to determine the full chemical shift tensor  $\delta$  is to perform NMR experiments on single crystals. In such experiments, a crystal of sufficient size is affixed to a goniometer axis (which commonly is oriented perpendicular to the external magnetic field  $\vec{B}_0$ ) and then rotated step-wise by an angle  $\varphi_i$ , with a spectrum being recorded for each orientation. To understand the number of resonances present in the  $^{207}\text{Pb}$  NMR spectra of vanadinite and pyromorphite, as shown in Fig. 5, one has to specify the number of crystallographically and magnetically non-equivalent lead atoms in the crystal structure. Since only atoms related by translational or inversion symmetry are magnetically equivalent, the  $6_3$  screw axis along the crystallographic  $c$ -axis generates three magnetically non-equivalent  $^{207}\text{Pb}$  at position  $6h$ , while the mirror planes parallel to the crystallographic  $ab$  plane generate two magnetically non-equivalent  $^{207}\text{Pb}$  at position  $4f$ . In summary, we expect to have a maximum of five signals in the respective  $^{207}\text{Pb}$  NMR spectra. For the rotation axes chosen by us, however,

both vanadinite and pyromorphite show four resolved resonances at most (see Fig. 6), albeit one with double intensity, belonging to the two  $^{207}\text{Pb}$  at Wyckoff position 4f. From the spectra in Fig. 5, the strong orientation dependency of the chemical shift becomes apparent. Plotting all resonance positions over a 180 degree rotation results in a so-called rotation pattern, as shown for pyromorphite in Fig. 6. The rotation of the tensor  $\delta$  causes the resonance frequencies to follow harmonic functions of the type (Volkoff et al. 1952):

$$\frac{\nu^k(\varphi_i)}{\nu_0} = A^k + B^k \cos 2\varphi_i + C^k \sin 2\varphi_i \quad (4)$$

Here, the factors  $A$ ,  $B$ ,  $C$  are combinations of the CS tensor elements, the exact form depending on the relative orientation of the tensor to the goniometer axis, and are generally different for each magnetically non-equivalent nuclide  $k$  in the unit cell.

By making use of the known symmetry relation between the lead atoms at positions 6h and 4f respectively, it is possible to fit the full  $^{207}\text{Pb}$  CS tensors, as well as the initially unknown orientation of the rotation axis (since the crystals were glued onto the goniometer in a random orientation) from only one rotation pattern (see Zeman et al. 2018 and Zeman et al. 2019). Although we need the data set shown in Fig. 7 primarily for discussing crystal morphology effects (see below), we decided to also re-determine the  $^{207}\text{Pb}$  CS tensors for pyromorphite from it. The details of this re-determination are given in the Supporting Information, with the resulting CS tensors listed in Table S1 being more precise than those reported in our original publication (Zeman et al. 2017).

## Relation of the $^{207}\text{Pb}$ chemical shift to crystal morphology

Referring back to Fig. 5, we note that the line widths of the  $^{207}\text{Pb}$  NMR signals, in each spectrum, differ significantly between pyromorphite and vanadinite. While vanadinite exhibits comparatively narrow, and constant line widths with a full width at half-maximum intensity (FWHM) of approximately 30 ppm, the  $^{207}\text{Pb}$  NMR signals in pyromorphite are inherently broader and are different for magnetically non-equivalent  $^{207}\text{Pb}$  atoms. Interestingly, for pyromorphite, the observed broadening also depends on the crystal orientation, as can be seen from the plots of FWHM vs. rotation angle in Fig. 7. By deconvoluting all resonances in a spectrum (see dotted lines in Fig. 5), FWHM was found to vary between 50 to 250 ppm for position 6*h* and between 28 to 42 ppm for position 4*f*. This variation of line width even appears to be systematically orientation-dependent, most obviously in the top left plot of Fig. 7. There are several factors influencing the line width of NMR spectra, starting with inherent transverse relaxation, and continuing with inhomogeneities of the static and the radiofrequency magnetic field, all of which however result in a constant line width in good approximation. It is different for broadening caused by spin couplings (see last term in Eq. (2)), which does contain orientation dependent terms (Laws et al. 2002, MacKenzie and Smith 2002). However, the coupling pattern of  $^{207}\text{Pb}$  in the apatite structure, being surrounded in the first coordination sphere by chlorine and oxygen only, is practically identical for vanadinite and pyromorphite, and cannot cause the large line width variation observed for the latter. We therefore attribute the orientation-dependent FWHM change shown in Fig. 7 to effects caused by macroscopic crystal imperfections, i.e. the well-documented mosaicity of single crystals (see, for example, Vinet et al. 2011).

The obvious question arising now is whether some quantitative information about the nature of this mosaicity may be derived from our NMR data. Mosaicity may be defined as an ensemble of small crystallites, which all have small deviations from a main orientation, which can be

described as the average of all crystallite orientations. For a simple first estimate of this effect in pyromorphite, this alignment deviation was assumed to follow a Gaussian distribution with a standard deviation angle  $\sigma$  along one of the crystallographic axes. The line width for a full rotation pattern was then calculated as the difference between the frequencies  $\nu^k(+\sigma)$  and  $\nu^k(-\sigma)$ , and adding a constant isotropic line width  $lw$  for each magnetically inequivalent lead atom<sup>3</sup>:

$$FWHM(\varphi) = |\nu^k(\varphi, \sigma) - \nu^k(\varphi, -\sigma) + lw| \quad (5)$$

Comparing the resulting line widths to the experimental results for each magnetically inequivalent <sup>207</sup>Pb atom, we found the best agreement for a distribution along the *c*-axis, with a standard deviation angle of  $\sigma = 5^\circ$ . For at least one lead site (top left plot of Fig. 7), the agreement between the prediction of this relatively crude model and the experimental data is remarkably good. It is also obvious from Fig. 7, however, that our simple model fails to completely reproduce the experimental results of all five lead sites. This can be easily understood by considering that mosaicity may also exist along other directions than just along the *c*-axis. Therefore, while the entire complexity of the actual disorder in our pyromorphite crystals could not be fully resolved here, the general approach shows the potential usefulness of NMR investigations for obtaining information about the geometry of multi-crystalline growth in minerals.

<sup>3</sup> A similar model has been used to quantify orientation-dependent line broadening in <sup>2</sup>H-NMR spectra of specifically deuterated azulene (C<sub>10</sub>H<sub>6</sub>D<sub>2</sub>). For such alignment disorder in a molecular crystal, the assumption of a Gaussian distribution worked very well (Bräuniger et al. 2000).

This usefulness of single-crystal NMR for characterization of crystal morphology can be further illustrated by the case of mimetite. In Fig. 8, the  $^{207}\text{Pb}$ -NMR spectra of two naturally grown crystals of mimetite are shown, which from optical inspection by polarizing microscope were assumed to be single crystals. One originates from China (Fig. 8; Mimetite A) with a size of approx.  $8 \times 5 \times 4 \text{ mm}^3$ , the other from Namibia (Fig. 8; Mimetite B) with a size of approx.  $1.3 \times 1 \times 1 \text{ mm}^3$ . Contrary to expectation, both spectra show more than the five  $^{207}\text{Pb}$  signals, which are the maximum allowed for a single crystal. At the same time, the observed spectra are markedly different from what would be expected from a polycrystalline powder sample representing all orientations, such as those shown in Fig. 2. Rather, the mimetite  $^{207}\text{Pb}$  spectra arise from a large, but “countable” number of differently oriented sub-crystals within the macroscopic agglomerates. Interestingly, from the fact that a higher number of resonances are resolved in the spectra of crystal A, it can be concluded that the actual number of crystallites in A is smaller, although its outer dimensions are much bigger than those of crystal B. In order to rationalize the appearance of the spectra of crystals A and B, we took the rotation patterns from our vanadinite specimen (which shows truly single crystalline behavior in terms of NMR) and pyromorphite (single crystalline, but with mosaicity effects on the NMR line width), and combined the  $^{207}\text{Pb}$  spectra for each orientation of the rotation pattern, which is equivalent to measuring 16 respectively 12 crystals in varying orientations simultaneously. The combined spectra (Fig. 8topleft; rotation spectra taken from Zeman et al. 2018, Fig. 8Bottomleft; rotation spectra from Fig. 6) look remarkably similar to the experimental  $^{207}\text{Pb}$ -NMR spectra of mimetite. This encourages the assumption that our crystal specimens of mimetite are condensed agglomerates of the order of 10 (crystal A) and 20 to 30 (crystal B) truly single crystalline domains, with more or less arbitrary orientation relative to each other. Thus, “sub-crystal counting” in multi-crystalline samples is in principle possible by solid-state NMR spectroscopy,

which, if quantitatively accomplished, could give additional information about the inner morphology of mineral agglomerates. The NMR approach is especially useful for large crystals with high absorption coefficients, such as present in lead-bearing minerals, where analysis of inner domain structure by X-ray diffractometry is practically impossible.

### **$T_1$ relaxation times of $^{207}\text{Pb}$**

The longitudinal relaxation time  $T_1$  is an important experimental parameter in NMR, since intensity distortions in the spectra may result from choosing repetition times too short. In the context of natural minerals,  $T_1$  values may also give indications about paramagnetic impurities, which would drastically shorten them. Such impurities could also have an effect on the NMR line width, impacting on our discussion of orientation-dependent line broadening in pyromorphite. We have therefore measured  $T_1$  for all minerals discussed here, with the results listed in Table 2, and measurement details given in the Supporting Information. Considering that the CS tensors of  $^{207}\text{Pb}$  in the minerals have appreciable anisotropy, the  $T_1$  values are remarkably long. At the same time, the observed relaxation times in the range of several seconds practically preclude the presence of paramagnetic impurities in all but trace concentrations, and also rule out noticeable effects on the observed line widths.

$T_1$	Vanadinite	Pyromorphite	Mimetite
$6h$	$(10.1 \pm 0.2) \text{ s}$	$(14.2 \pm 0.8) \text{ s}$	$(8.6 \pm 0.6) \text{ s}$
$4f$	$(5.1 \pm 0.1) \text{ s}$	$(5.1 \pm 0.1) \text{ s}$	$(5.2 \pm 0.8) \text{ s}$

**Table 2.** Longitudinal relaxation times of  $^{207}\text{Pb}$  at the position  $6h$  and  $4f$  in the apatite structure of vanadinite and pyromorphite (single-crystal NMR), and mimetite (MAS NMR).

## Experimental Section

Single-crystal NMR spectra were acquired with a Bruker Avance-III 400 spectrometer at MPI-FKF Stuttgart, with the Larmor frequency being  $\nu_0(^{207}\text{Pb}) = 83.71$  MHz. The spectra were recorded with echo acquisition (3/6  $\mu\text{s}$ ) to minimize base line roll (Kunwar 1986), using a recycle delay of 60 s, and referenced to  $\text{Pb}(\text{NO}_3)_2$  powder at -3487.5 ppm. The goniometer probe with solenoid coil was built by NMR Service GmbH (Erfurt, Germany). For the MAS spectra, a polycrystalline sample was created by crushing macroscopic crystals of mimetite with an agate mortar. The MAS spectra were acquired on a Bruker Avance-III 500 spectrometer at LMU Munich, using a 2.5 mm rotor for lead with  $\nu_0(^{207}\text{Pb}) = 104.63$  MHz. The global fit of the rotation pattern data for the chemical shift tensor of  $^{207}\text{Pb}$  in pyromorphite, and the deconvolution of the static  $^{207}\text{Pb}$  NMR spectra, was performed using the program Igor Pro 7.08 from WaveMetrics Inc.

## Implications

Our results for  $^{207}\text{Pb}$  in vanadinite, pyromorphite, and mimetite suggest that single crystal NMR spectroscopy provides not only information about the relevant NMR interaction tensors, i.e. the chemical shift, but also information about local coordination geometry and crystal microstructure. Regarding the relation between  $^{207}\text{Pb}$  chemical shift and crystal structure parameters, the correlations to both unit cell volume and oxygen proximity shown here could possibly be extended to other lead bearing minerals and/or apatites. This could result in the establishment of more reliable and widely applicable correlations between NMR interaction parameters and structural features. Similarly, the information on crystal morphology available via NMR spectroscopy, as discussed herein, opens an alternative venue to methods like optical microscopy,

X-ray diffraction, and SEM/Electron Backscatter Diffraction to study effects such as mosaicity and multi-crystalline structures, notably if the sample is in the millimetre size range and cannot be destroyed for analysis. A systematic, rather than a random pattern of misorientation in the crystal microstructure is represented by twinning. Work to characterize twinning in macroscopic crystals (i.e., the number of twin domains and their relative orientation) by NMR spectroscopy is currently in progress in our laboratory.

## References Cited

- Andrew, E.R. (1981) Magic angle spinning in solid state n.m.r. spectroscopy. Philosophical Transactions of the Royal Society A, 299, 505-520, <https://doi.org/10.1098/rsta.1981.0032>.
- Anet, F.A.L., O'Leary, D.J. (1991) The shielding tensor. Part I: Understanding its symmetry properties. Concepts in Magnetic Resonance, 3, 193-214, <https://doi.org/10.1002/cmr.1820030403>.
- Bak, M., Rasmussen, J. T., Nielsen, N. C. (2000) SIMPSON: A general simulation program for solid-state NMR spectroscopy. Journal of Magnetic Resonance, 147, 296-330, <https://doi.org/10.1006/jmre.2000.2179>.
- Bräuniger, T., Poupko, R., Luz, Z., Gutsche, P., Meinel, C., Zimmermann, H., Haeberlen, U. (2000) The dynamic disorder of azulene: A single crystal deuterium nuclear magnetic resonance study. Journal of Chemical Physics, 112, 10858-10870, <https://doi.org/10.1063/1.481727>.
- Chopard, B., Herrmann, H.J., Vicsek, T. (1991) Structure and growth mechanism of mineral dendrites. Nature, 353, 409-412, <https://doi.org/10.1038/353409a0>.
- Epp, T., Marks, M.A.W., Ludwig, T., Kendrick, M.A., Eby, N., Neidhart, H., Oelmann, Y., Markl, G. (2019) Crystallographic and fluid compositional effects on the halogen (Cl, F, Br, I) incorporation in pyromorphite-group minerals. American Mineralogist, 104, 1673-1688, <https://doi.org/10.2138/am-2019-7068>.
- Galwey, A.K., Jones, K.A. (1963) An Attempt to Determine the Mechanism of a Natural Mineral-forming Reaction from Examination of the Products. Journal of the Chemical Society, 0, 5681-5686, <https://doi.org/10.1039/JR9630005681>.
- Haeberlen, U. (1976) High resolution NMR in solids: Selective averaging. Advanced Magnetic Resonance, Ed. J. Waugh, Academic Press, New York.
- Harris, R.K., Sebald, A. (1987) Experimental Methodology for High-Resolution Solid-State NMR of Heavy-Metal Spin- $\frac{1}{2}$  Nuclei. Magnetic Resonance in Chemistry, 25, 1058-1062, <https://doi.org/10.1002/mrc.1260251208>.



- Harris, R.K. (2004) NMR Crystallography: The use of chemical shifts. *Solid State Sci.*, 6, 1025-1037, <https://doi.org/10.1016/j.solidstatesciences.2004.03.040>.
- Herzfeld, J., Berger, A.E. (1980) Sideband intensities in NMR spectra of samples spinning at the magic angle. *The Journal of Chemical Physics*, 73, 6021-6030, <https://doi.org/10.1063/1.440136>.
- Kunwar, A.C., Turner, G.L., Oldfield, E. (1986) Solid-state spin-echo Fourier transform NMR of <sup>39</sup>K and <sup>67</sup>Zn salts at high field. *Journal of Magnetic Resonance*, 69, 124-127, [https://doi.org/10.1016/0022-2364\(86\)90224-6](https://doi.org/10.1016/0022-2364(86)90224-6).
- Laws, D.D., Bitter, H.-M.L., Jerschow, A. (2002) Solid-State NMR Spectroscopic Methods in Chemistry. *Angewandte Chemie International Edition*, 41, 3096-3129, [https://doi.org/10.1002/1521-3773\(20020902\)41:17<3096::AID-ANIE3096>3.0.CO;2-X](https://doi.org/10.1002/1521-3773(20020902)41:17<3096::AID-ANIE3096>3.0.CO;2-X).
- MacKenzie, K.J.D., Smith, M.E. (2002) Multinuclear Solid-State NMR of Inorganic Materials. Pergamon Materials Series Vol. 6, Ed. R.W. Cahn, Elsevier Science, Oxford.
- Okudera, H. (2013) Relationships among channel topology and atomic displacements in the structures of Pb<sub>5</sub>(BO<sub>4</sub>)<sub>3</sub>Cl with B = P (pyromorphite), V (vanadinite), and As (mimetite). *American Mineralogist*, 98, 1573-1579, <https://doi.org/10.2138/am.2013.4417>.
- Otálora, F., Garcia-Ruiz, J. (2014) Nucleation and growth of the Naica giant gypsum crystals. *Chemical Society Reviews*, 43, 2013-2026, <https://doi.org/10.1039/C3CS60320B>.
- Penn, R.L., Banfield, J.F. (1999) Morphology development and crystal growth in nanocrystalline aggregates under hydrothermal conditions: Insights from titania. *Geochimica et Cosmochimica Acta*, 63(10), 1549-1557, [https://doi.org/10.1016/S0016-7037\(99\)00037-X](https://doi.org/10.1016/S0016-7037(99)00037-X).
- Vinet, N., Flemming, R.L., Higgins, M.D. (2011) Crystal structure, mosaicity, and strain analysis of Hawaiian olivines using in situ X-ray diffraction. *American Mineralogist*, 96, 486-497, <https://doi.org/10.2138/am.2011.3593>.
- Volkoff, G.M., Petch, H.E., Smellie, D.W.L. (1952) Nuclear Electric Quadrupole Interaction in Single Crystals. *Canadian Journal of Physics*, 30, 270-289, <https://doi.org/10.1139/p52-026>.
- Zeman, O.E.O., Hoch, C., Hochleitner, R., Bräuniger, T. (2018) NMR interaction tensors of <sup>51</sup>V and <sup>207</sup>Pb in vanadinite, Pb<sub>5</sub>(VO<sub>4</sub>)<sub>3</sub>Cl, determined from DFT calculations and single-crystal NMR measurements, using only one general rotation axis. *Solid State Nuclear Magnetic Resonance*, 89, 11-20, <https://doi.org/10.1016/j.ssnmr.2017.12.002>.
- Zeman, O.E.O., Moudrakovski, I.L., Hoch, C., Hochleitner, R., Schmahl, W.W., Karaghiosoff, K., Bräuniger, T. (2017) Determination of the <sup>31</sup>P and <sup>207</sup>Pb Chemical Shift Tensors in Pyromorphite, Pb<sub>5</sub>(PO<sub>4</sub>)<sub>3</sub>Cl, by Single-Crystal NMR Measurements and DFT calculations. *Zeitschrift für anorganische und allgemeine Chemie*, 643, 1635-1641, <https://doi.org/10.1002/zaac.201700261>.
- Zeman, O.E.O., Steinadler, J., Hochleitner, R., Bräuniger, T. (2019) Determination of the Full <sup>207</sup>Pb Chemical Shift Tensor of Anglesite, PbSO<sub>4</sub>, and Correlation of the Isotropic Shift to Lead-Oxygen Distance in Natural Minerals. *Crystals*, 9(1), 43, <https://doi.org/10.3390/cryst9010043>.

## List of Captions

**Figure 1.** (a) Crystals of vanadinite,  $\text{Pb}_5(\text{VO}_4)_3\text{Cl}$ , from Mibladen, Morocco. (b) Crystals of pyromorphite,  $\text{Pb}_5(\text{PO}_4)_3\text{Cl}$ , from Grube Friedrichsseggen near Bad Ems, Germany (mineralogical state collection inventory no. 3013). (c) Crystals of mimetite,  $\text{Pb}_5(\text{AsO}_4)_3\text{Cl}$ , from China.

**Figure 2.** (a) Simulated  $^{207}\text{Pb}$  static powder spectra of pyromorphite with Wyckoff position  $6h$  and  $4f$  shown combined, and (b) as separate contributions. (c) Simulated  $^{207}\text{Pb}$  magic-angle spinning spectra of pyromorphite at 110kHz, and (d) 11kHz spinning speed, with the isotropic bands for Wyckoff position  $6h$  (-2170 ppm) and  $4f$  (-2813 ppm) indicated. All spectra were calculated with the SIMPSON package (Bak et al. 2000), using the chemical shift values from Table S1. (Note that static and MAS spectra are plotted on different intensity scales, since the spinning side bands in the MAS spectra contain the accumulated intensity of many powder orientations and hence have much higher signal intensity than the broad static spectra.)

**Figure 3.** Magic-angle spinning  $^{207}\text{Pb}$ -NMR of polycrystalline mimetite,  $\text{Pb}_5(\text{AsO}_4)_3\text{Cl}$ , at 20 kHz spinning speed, with the isotropic bands for Wyckoff position  $6h$  (-2074 ppm) and  $4f$  (-2124 ppm) indicated. The spectrum was acquired in a magnetic field of  $B_0 = 11.7$  T with 2160 scans and a recycle delay of 60 s.

**Figure 4.** Left: Unit cell of mimetite according to Okudera 2013, viewed down the  $b$  axis to illustrate the  $c/a$  ratio. The chlorine atoms are shown in green, the Pb atoms at Wyckoff position  $4f$  in dark purple, Pb atoms at position  $6h$  in purple, and the As atoms in dark green tetrahedrally coordinated by oxygen (red). Right:  $^{207}\text{Pb}$  NMR isotropic chemical shifts of vanadinite (red), pyromorphite (blue), and mimetite (green) versus the respective  $c/a$  ratio, with the least-square fit (dashed line) showing good linear correlation. Lead atoms at position  $6h$  are shown as hexagons and as squares at position  $4f$ .

**Figure 5.** Left:  $^{207}\text{Pb}$  NMR spectra of a single crystal of vanadinite,  $\text{Pb}_5(\text{VO}_4)_3\text{Cl}$ , rotated counter-clockwise by the indicated angle  $\varphi$  around a rotation axis perpendicular to the external magnetic field  $B_0$ . Right:  $^{207}\text{Pb}$  NMR spectra of a single crystal of pyromorphite,  $\text{Pb}_5(\text{PO}_4)_3\text{Cl}$ , acquired by the same procedure. For the orientations of 75/165 degrees, the dashed lines show the deconvolution of each signal with a Lorentzian fit. The colors of the Lorentzian fits correspond to those of the harmonics in Fig. 6.

**Figure 6.** Full rotation pattern over  $180^\circ$  of pyromorphite,  $\text{Pb}_5(\text{PO}_4)_3\text{Cl}$ , for the 3 magnetically non-equivalent  $^{207}\text{Pb}$  at Wyckoff position  $6h$ , and 2 (unresolved) non-equivalent  $^{207}\text{Pb}$  at position  $4f$ . The pyromorphite crystal is rotated step-wise by  $15^\circ$  around an axis perpendicular to the external magnetic field  $B_0$ .

**Figure 7.** Experimental full width at half-maximum intensities (FWHM) for the full rotation pattern over 180° of pyromorphite,  $\text{Pb}_5(\text{PO}_4)_3\text{Cl}$ , for the 3 magnetically non-equivalent  $^{207}\text{Pb}$  at Wyckoff position 6*h* (hexagons), and 2 (non-resolved) non-equivalent  $^{207}\text{Pb}$  at position 4*f* (squares). The solid lines were calculated for a Gaussian distribution of crystal domains about the *c* axis with  $\sigma = 5^\circ$ , see text for details.

**Figure 8.** Top Left: Added up  $^{207}\text{Pb}$  NMR signals of the full rotation pattern of vanadinite, presented by Zeman et al. 2018. Top Right:  $^{207}\text{Pb}$  NMR spectra of a supposed single crystal of mimetite (crystal A) from China. Bottom Left: Added up  $^{207}\text{Pb}$  NMR signals of the full rotation pattern of pyromorphite (Fig. 3). Bottom Right:  $^{207}\text{Pb}$  NMR spectra of a supposed single crystal of mimetite (crystal B) from Tsumeb, Namibia (mineralogical state collection inventory no. 4770).

## List of Figures

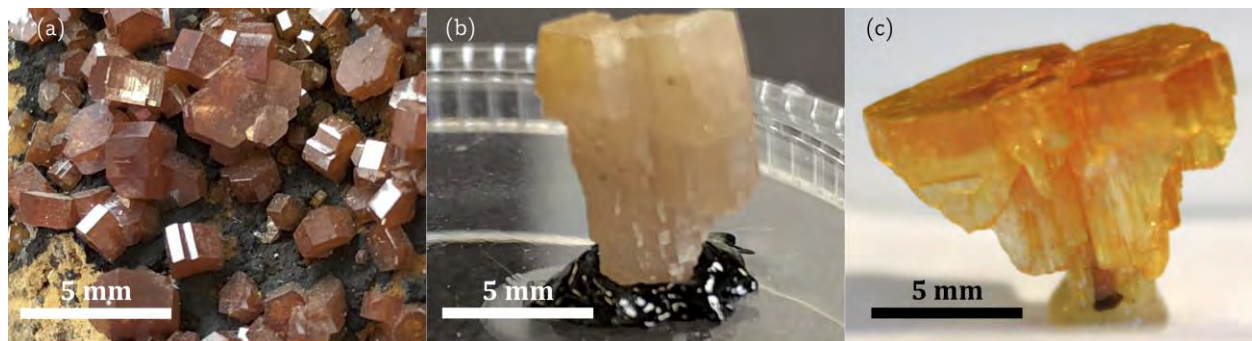


**Figure 1.**

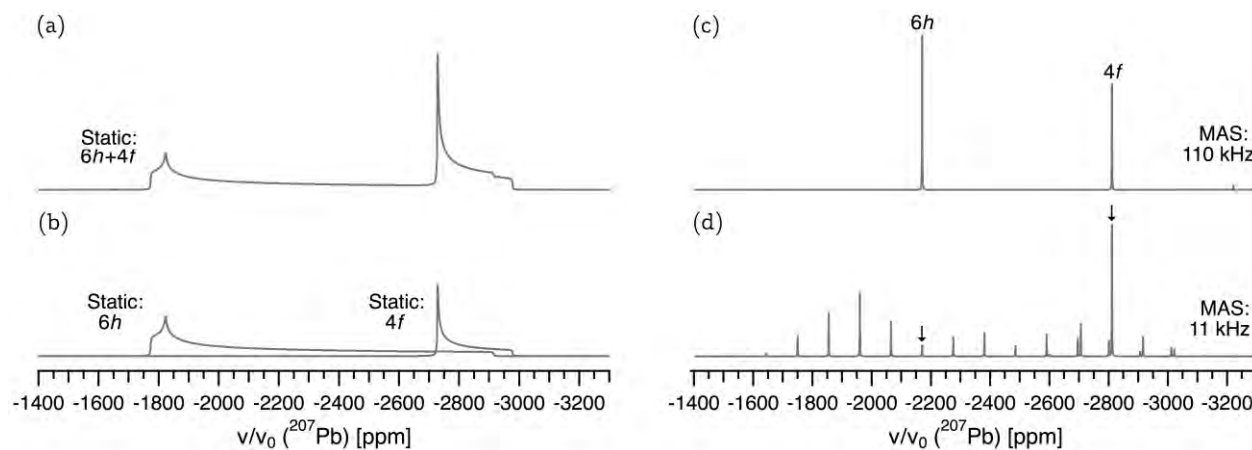


**Figure 2.**

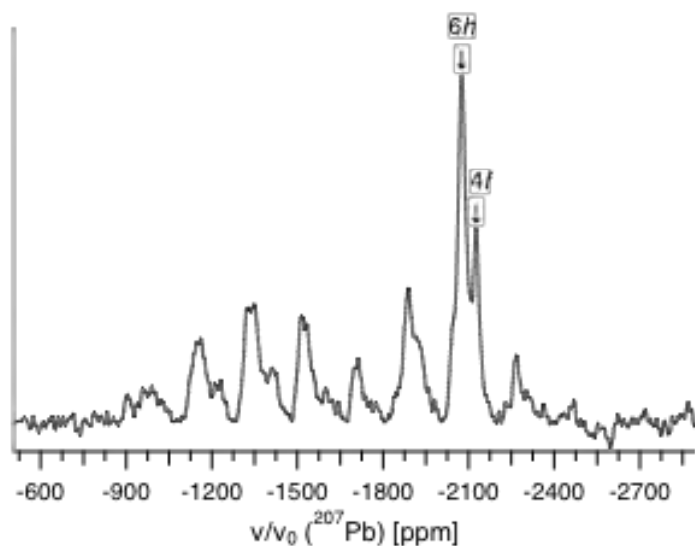


Figure 3.

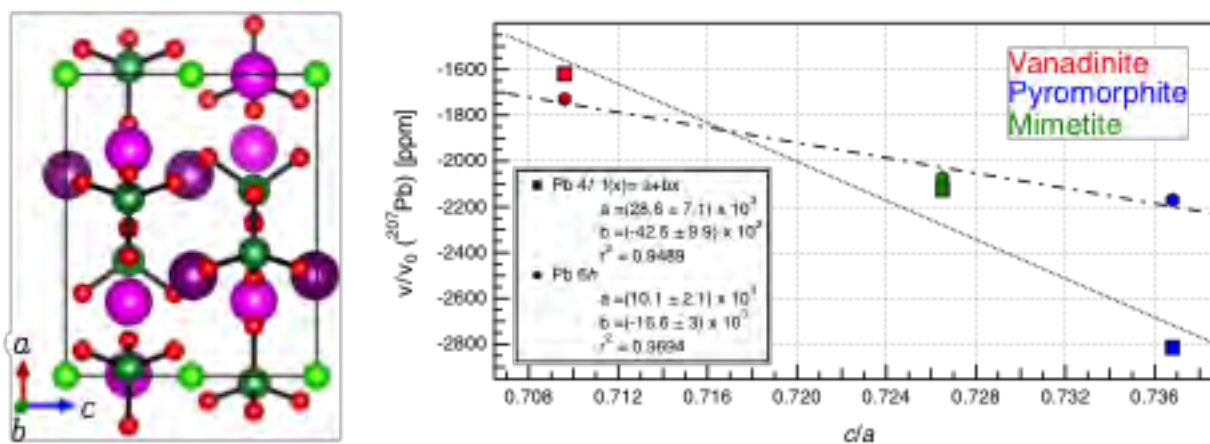


Figure 4.

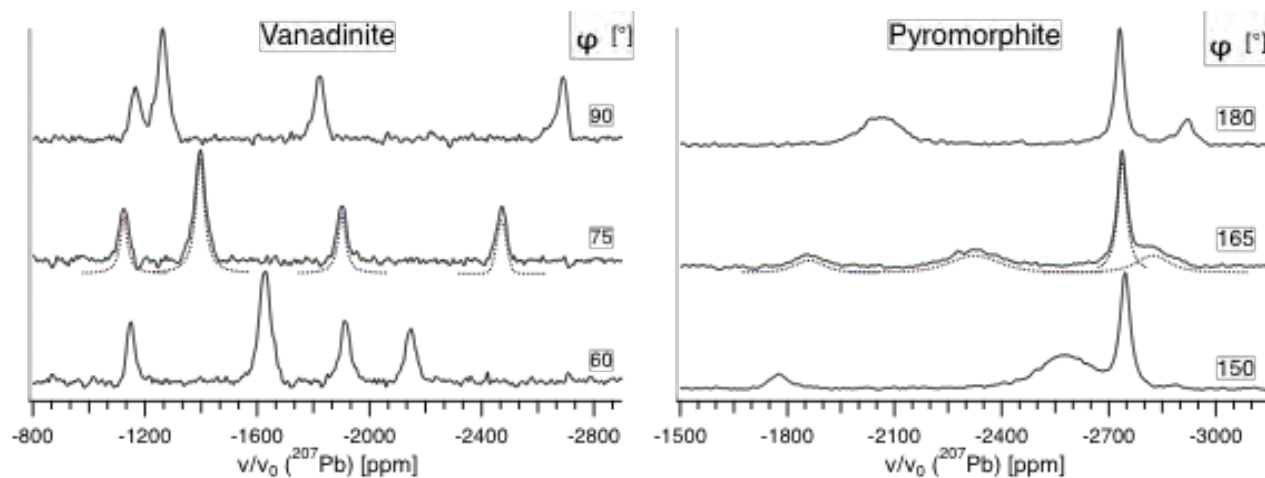


Figure 5.

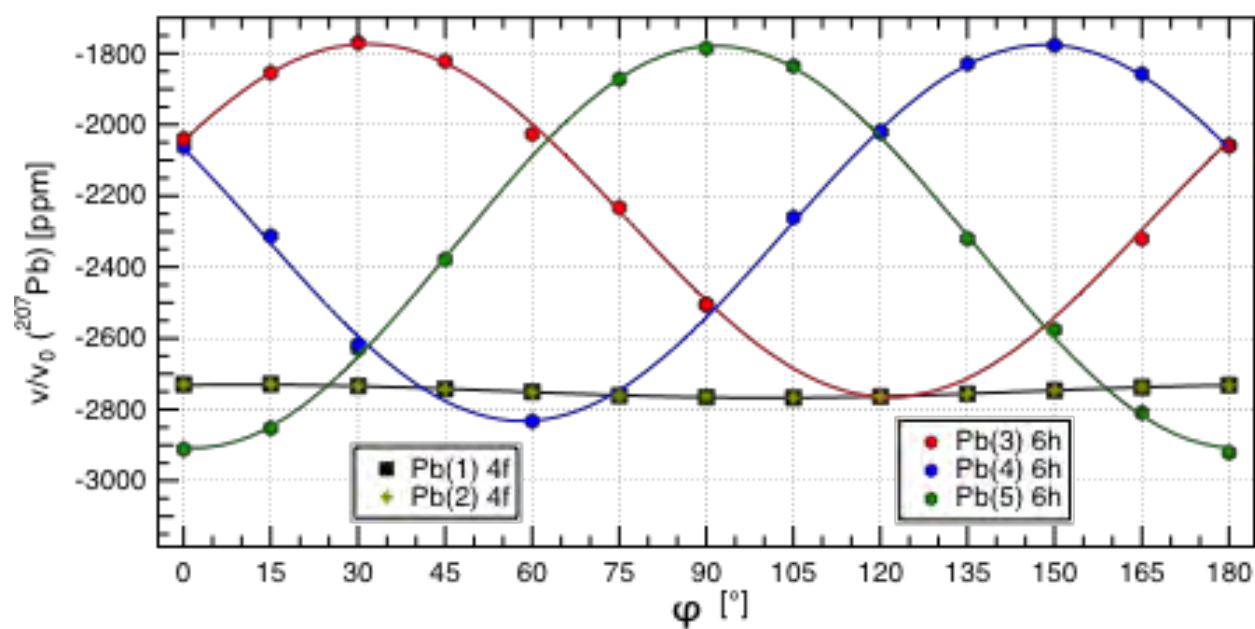


Figure 6.

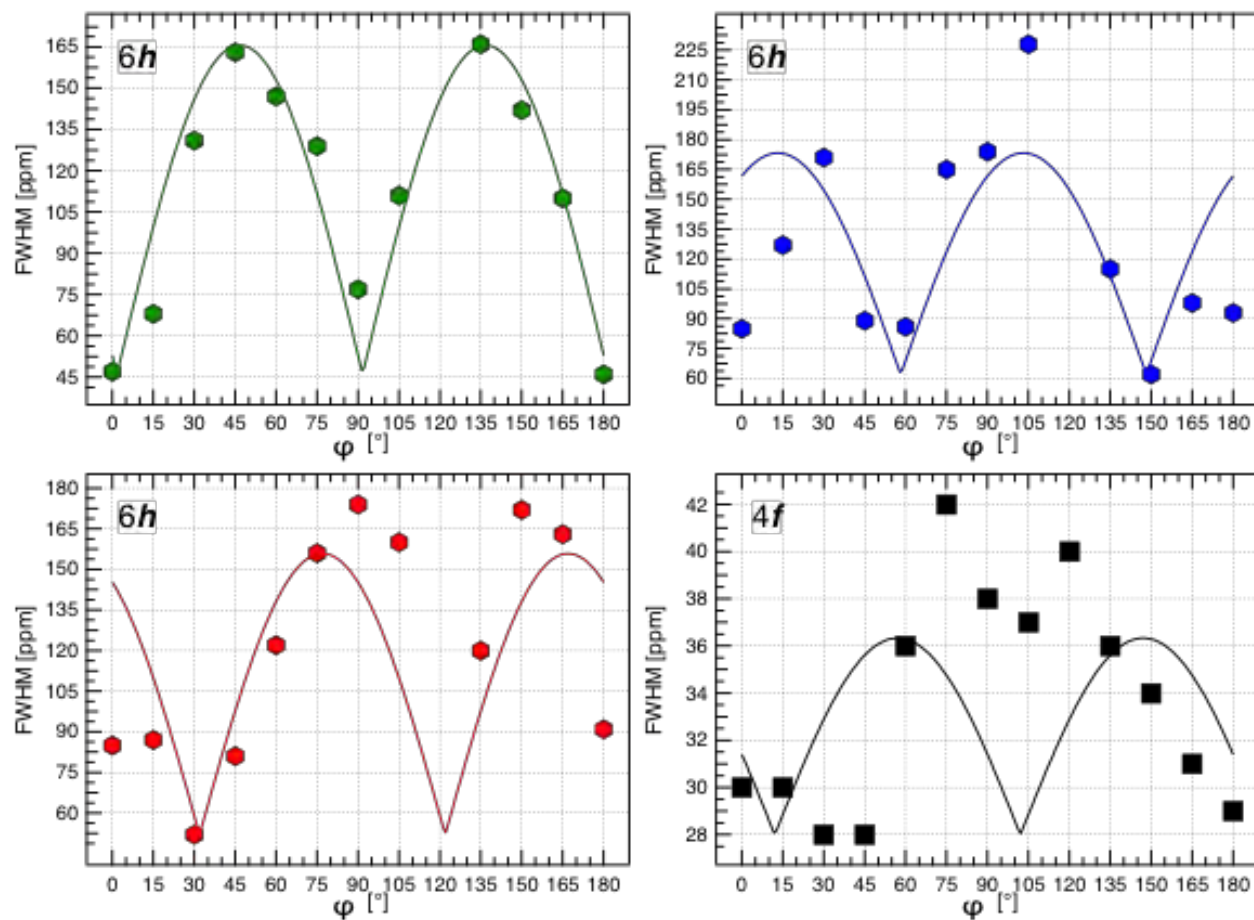
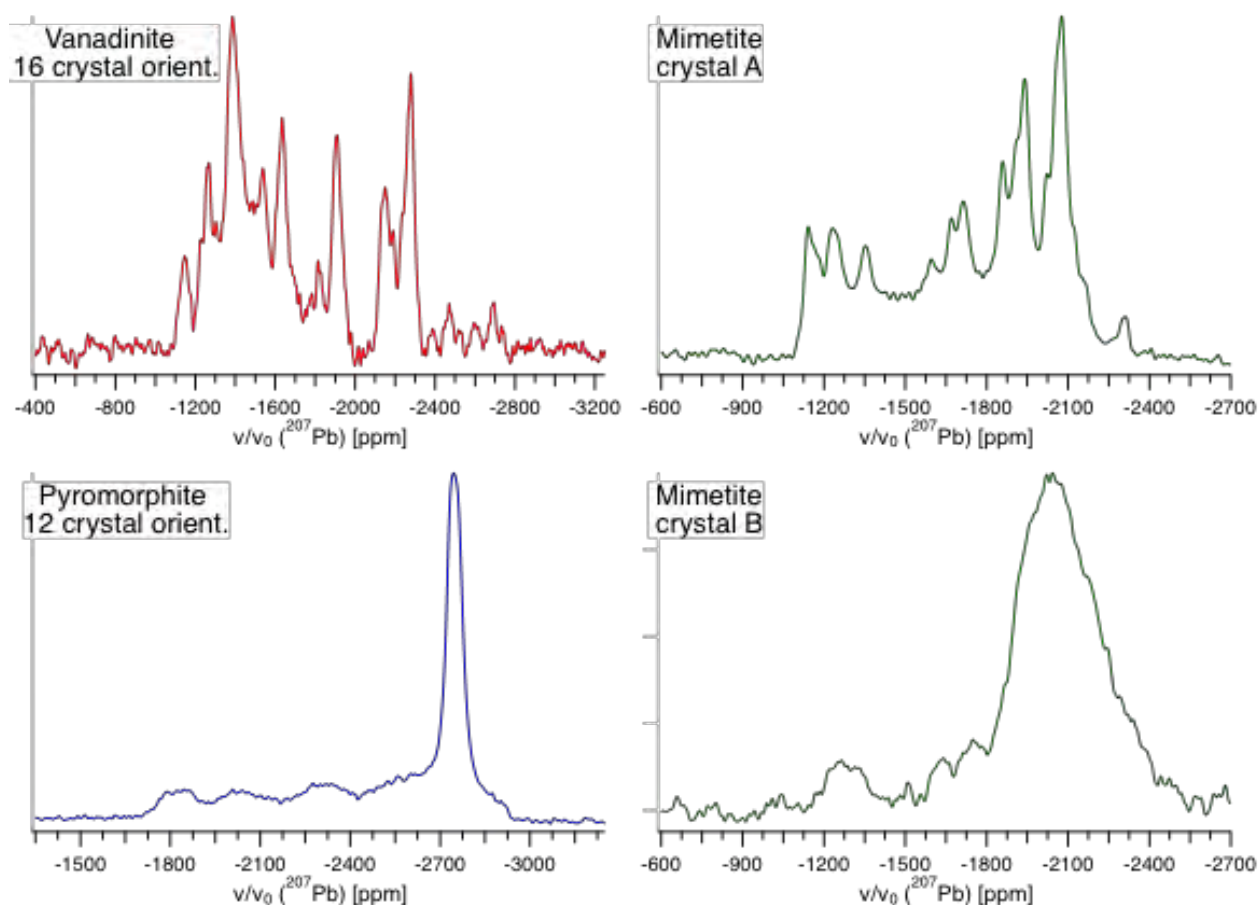


Figure 7.



**Figure 8.**